




# Highly active visible-light-driven photo-electrocatalytic process in TiO<sub>2</sub>/Ti electrode by Te doping

Muhammad Nurdin<sup>1</sup> · Muhammad Zakir Muzakkar<sup>1</sup> · Maulidiyah Maulidiyah<sup>1</sup> · Cici Sumarni<sup>1</sup> · Thamrin Azis<sup>1</sup> · Ratna Ratna<sup>2</sup> · Muhammad Natsir<sup>1</sup> · Irwan Irwan<sup>1,4</sup> · La Ode Agus Salim<sup>1,5</sup> · Akrajas Ali Umar<sup>3</sup> 

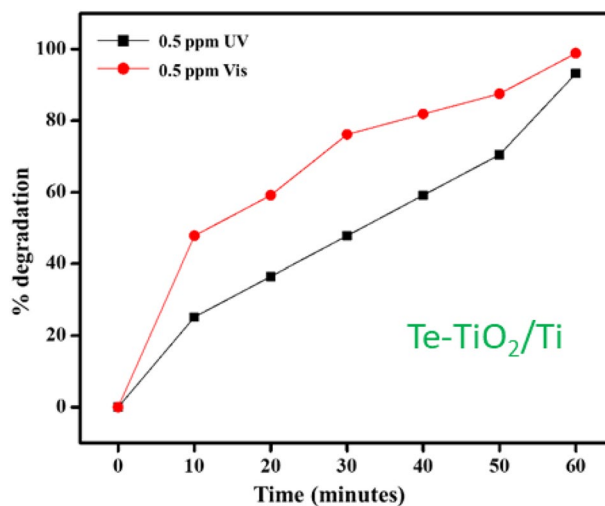
Received: 4 May 2022 / Accepted: 24 September 2022  
© The Author(s), under exclusive licence to Springer Nature B.V. 2022

## Abstract

The concern over increasing environmental contamination by dye agents from textile industries, such as Reactive yellow 105, requires a special catalyst that can rapidly and effectively eradicate the dye chemical. Here, we demonstrate a new design of catalyst, i.e., Te doped TiO<sub>2</sub>/Ti composite electrode, that promotes highly active charge transfer with the Reactive yellow 105 dye for efficient photoelectrocatalytic degradation under visible light irradiations. Our results show that the new photocatalyst effectively degrades up to 90% of 0.5 ppm of the Reactive yellow 105 dye under visible light irradiation within 60 min, which is equivalent to the degradation rate constant of 0.0611 M<sup>-1</sup> min<sup>-1</sup>. It is impressively higher than the pristine photocatalyst (TiO<sub>2</sub>/Ti) of which it only degrades 70 and 65% of dye compound under UV and Vis irradiation respectively or equivalent to degradation kinetic rate as low as 0.037 and 0.0361 M<sup>-1</sup> min<sup>-1</sup>, respectively. The degradation of dye compound is enhanced to 100% when the new catalyst is applied in photoelectrocatalytic degradation process under visible light irradiation or approximately 95% degradation under UV light irradiation. The Te doped TiO<sub>2</sub>/Ti photoelectrocatalyst can be a new platform for rapid Reactive yellow 105 dye contamination in the environment.

## Graphical abstract

Te doping enhances visible photoactivity of TiO<sub>2</sub> nanotube on Ti electrode.



**Keywords** Photoelectrocatalysis · Te doped TiO<sub>2</sub>/Ti electrode · Reactive yellow 105 · Catalytic degradation

Extended author information available on the last page of the article

## 1 Introduction

The increasing growth of the textile industry has caused a critical impact on the quality of the environment, due to improper disposal of their liquid waste. The liquid waste includes dyestuffs, a non-biodegradable organic compound containing azo compounds, and is highly carcinogenic [1–3]. One of the common dyes contamination is from Reactive yellow 105 [ $C_{44}H_{24}C_{12}N_{14}Na_6O_{20}S_6$ ], a dye that is made from azo compounds and its derivatives of which are benzene groups. Reactive yellow, just like the name, is a yellow synthetic coloring agent that is hazardous if inhaled, exposed to skin and eyes, or ingested. The health effects can be irritation to breathing, skin irritation, eye irritation, and cancer [4, 5]. If ingested, it can cause nausea, vomiting, abdominal pain, diarrhea, heat, and low blood pressure. Further consequences can lead to bladder cancer [6]. Therefore, Reactive yellow waste substances need to be processed before being released into the environment [7, 8].

A simple and effective way to treat environmental pollution from dye agents is via a photolysis process using artificial or sunlight UV light irradiation. However, the dye degradation can be accelerated when photocatalyst, a semiconducting oxides material, is employed. During the photolysis or photocatalysis process, dye decomposes into simpler components that are safer for the environment [9]. One of the semiconducting oxide materials that have been widely explored as a photocatalyst is titanium dioxide ( $TiO_2$ ) [10, 11]. This material exhibits a high chemical and physical stability, is non-toxic, relatively inexpensive, and has higher photocatalyst capability compared to other types of semiconducting materials [12, 13]. Owing to its excellent photocatalytic properties, titanium dioxide ( $TiO_2$ ) has been extensively used for microorganism inactivation, anti-fog, and self-cleaning [14]. In many processes,  $TiO_2$  demonstrates a dual function in dye degradation, namely as an adsorbent and photocatalyst [15, 16], making this material become the subject of active study for environmental contamination mitigation.

The degradation capability of  $TiO_2$  depends on the phase crystallinity it has. The anatase phase is recognized as the most photocatalytically active crystalline form of  $TiO_2$ . However, it has a critical weakness that is it is only active if exposed to UV light irradiation with a wavelength corresponding to its bandgap energy of 3.2 eV, limiting its applicability [17, 18].

Nevertheless, its photoactivity can be modified by doping  $TiO_2$  with different cations or anions into its crystal lattice [19–21]. In many cases, the doping process can improve the  $TiO_2$  activity in the visible light region and prolong the carrier lifetime, reducing the recombination

between electrons and holes [22–25]. However, doping  $TiO_2$  with metal ions in most cases causes thermal instability and increases defect density that plays a key role as the recombination center in the material. Therefore, the use of doping that improves the photoactivity and at the same time augments the photocatalytic properties of anatase  $TiO_2$  is demanded expanded photocatalytic degradation of dye contamination. Here, we design a new photoelectrocatalyst system, i.e., Te doped  $TiO_2/Ti$  nanocomposite, and evaluate its photoactivity under UV and visible light irradiation. Chalcogenide, in the form of glasses, has exhibited peculiar performance in thermoelectrics, solar cells, and photocatalysis applications [10, 26]. Tellurium (Te) is amongst the most potential system for doping  $TiO_2$  as it also has antibacterial activity as a result of its strong oxidative properties so that it is very potential as a photocatalyst  $TiO_2$  doping material to degrade Reactive yellow 105. Its narrow bandgap, namely  $E_{bg} = 0.32$  eV [27, 28], and p-type conductivity may drive visible photoactivity in  $TiO_2$  photocatalyst. We found that the Te– $TiO_2/Ti$  electrode can accelerate the degradation of Reactive yellow 105 dye, which is remarkably faster if compared with that the undoped system. In the typical process, the Te doped  $TiO_2/Ti$  electrode can completely degrade 0.5 ppm Reactive yellow 105 dye within 60 min of photoelectrocatalytic reaction under visible light irradiation and 95% degradation under UV light irradiation. Meanwhile, it is only 92 and 70% in pristine  $TiO_2/Ti$  electrodes under UV and visible light irradiation respectively. We thought that the enhancement of the photoelectrocatalytic degradation of dye molecules is the result of photocarrier lifetime improvement in  $TiO_2$  upon being doped with Te, realizing active electron transfer between catalyst and dye molecules for dye molecules degradation [10, 29, 30]. The Te doped  $TiO_2/Ti$  photoelectrocatalyst can be a new platform for rapid Reactive yellow 105 dye contamination in the environment.

## 2 Experimental

### 2.1 Preparation of Te doped $TiO_2/Ti$ electrode

The Te doped  $TiO_2/Ti$  electrode preparation was initiated by firstly preparing  $TiO_2$  on Ti electrode via an anodizing process. A Ti plate of length, width, and thickness of 2, 0.5, 0.1 cm, respectively, purchased from Merck, the USA was used in this study. During the anodizing process, the Ti plate functioned as the anode. Meanwhile, the cathode was Cu. We used glycerol electrolyte solution and  $NH_4F$  0.27 M in this process. The two electrodes were connected to a 25 V direct current (DC) bias for the anodizing process for 4 h. From this process,  $TiO_2$  thin film will form on the surface of the Ti electrode. The

sample was then calcined in air at 500 °C for 1.5 h to obtain the anatase crystal structure of TiO<sub>2</sub>.

After that, Te doped TiO<sub>2</sub>/Ti electrode was prepared by dipping the TiO<sub>2</sub>/Ti electrode into sol-gel containing Te. Sol-gel was synthesized by mixing 4.0 mL of titanium tetra isopropoxide (TTIP), ethanol as a solvent, aquades, and 1.0 mL acetic acid. The reaction was refluxed for 3 h at 50 °C [2, 31]. The addition of acetic acid was to control the rate of hydrolysis and to help the pore formation in the obtained sol. Finally, Te doping was carried out by adding 4.0 mL of Te(OH)<sub>6</sub> tellurium acid into the sol and stirring at 500 rpm at 50 °C. White sol-gel was produced from this process after following solvent evaporation. Te doped TiO<sub>2</sub>/Ti electrode was then prepared by dipping the TiO<sub>2</sub>/Ti electrode into the sol-gel and then annealed in air at 150 °C for 1.5 h. All chemicals were purchased from Merck, USA, and used directly without purification.

## 2.2 Characterizations

The phase crystallinity of the sample was examined using X-ray diffraction spectroscopy Bruker D8 XRD spectrometer with CuK $\alpha$  irradiation and scan rate 2°/min. The morphology of the sample was characterized using field-emission scanning electron microscopy FESEM Zeiss Supra 55VP FESEM model with a resolution of 1.0 nm operated at 30 kV, which is equipped with energy dispersive X-ray (EDX) for elemental analysis. The nature of Te doping in the sample was also evaluated using Fourier transform infrared spectroscopy (FTIR).

## 2.3 Photoelectrocatalytic degradation of dye

Photoelectrocatalytic degradation of Reactive yellow 105 dye was evaluated using a three-electrode electrochemical system with Te doped TiO<sub>2</sub>/Ti electrode as working electrode, Cu plate as the counter electrode, and Ag/AgCl as the reference electrode. The system was biased with a direct current of 0.4 V and operated under Multi-Pulse Amperometry (MPA). Visible light of power 18 Watts from Xenon lamp and UV of wavelength 360 nm from Mercury lamp with a power of 15 Watts and were used as a light source during the photoelectrocatalytic process. The degradation of Reactive yellow 105 dye was examined by mean of optical absorption spectroscopy using UV-Vis spectrometer Winlab optical spectrophotometer.

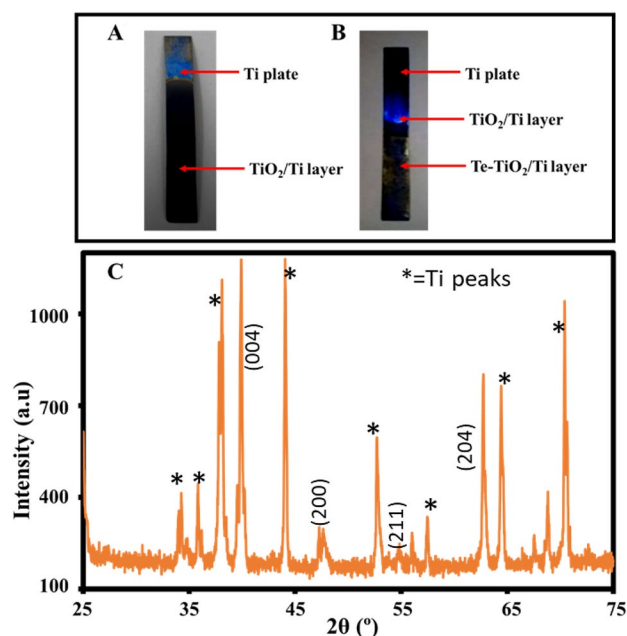
## 3 Results and discussion

### 3.1 Te doped TiO<sub>2</sub>/Ti electrode

The Te doped TiO<sub>2</sub>/Ti electrode has been successfully prepared in this study. The preparation process was initiated

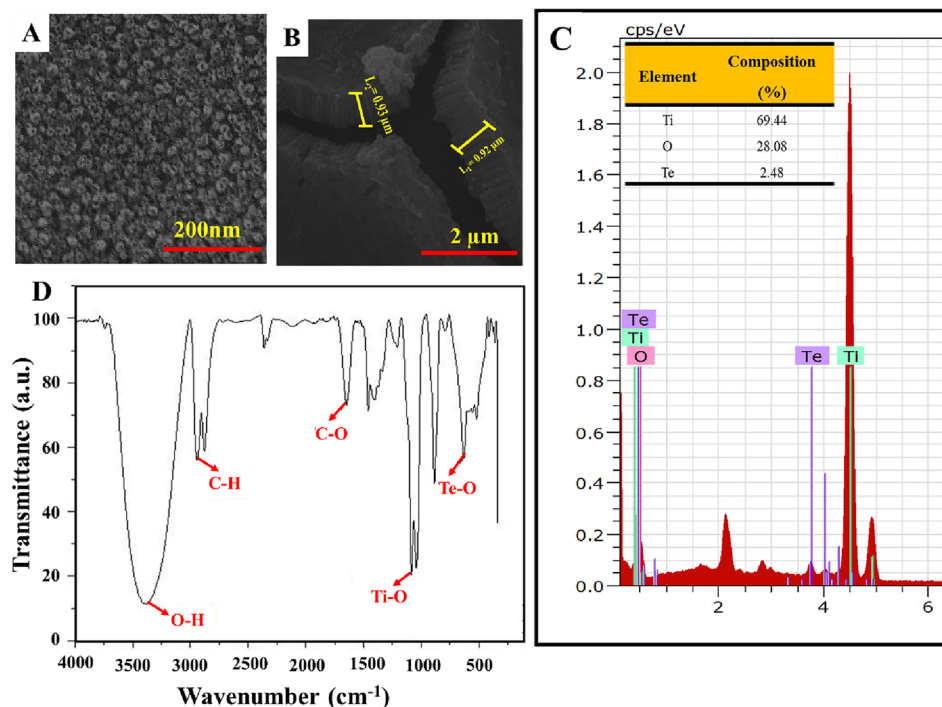
with the synthesis of TiO<sub>2</sub> films on the surface of the Ti plate electrode that was achieved via the anodizing method. Figure 1B shows the typical optical photographic image of the electrode after anodizing and after deposition of Te doped TiO<sub>2</sub> layer. As Fig. 1A reveals, a solid-black-colored film effectively covers the Ti plate electrode. XRD analysis result (Fig. 1C) verifies that the film is anatase TiO<sub>2</sub> where the XRD pattern of peaks  $2\theta$  of 38°, 47°, and 55° agrees with JCPDS no 96-153-4879 for anatase TiO<sub>2</sub>. These peaks are associated with (0 0 4), (2 0 0), and (2 1 1) Bragg planes, respectively. The black color of the film is the result of efficient visible light absorption by the highly porous surface of TiO<sub>2</sub> films as judged from FESEM analysis that will be discussed later. Figure 1C shows the typical image of the Te doped TiO<sub>2</sub> layer on top of TiO<sub>2</sub>/Ti films. A yellowish-black colored film is observed, an indication of the new layer, i.e., Te doped TiO<sub>2</sub>, is successfully deposited on the electrode. The verification of the existence of the process is conducted via EDX and FTIR analysis that will be discussed later.

Figure 2 shows the typical FESEM image of the TiO<sub>2</sub> and Te doped TiO<sub>2</sub> films on the Ti electrode. As has been mentioned earlier, the TiO<sub>2</sub> film on the Ti electrode exhibits a highly porous morphology that is constructed by a large density of the tubular structure of diameter approximately 500 nm (Fig. 2A). This surface morphology is the origin of the black-colored image of the films in which the light is effectively absorbed by the porous structure, reflecting a dark image to the eye. This surface morphology should



**Fig. 1** Optical image of TiO<sub>2</sub> layer on titanium plate surface after following anodization process (A) and Te-TiO<sub>2</sub>/Ti electrode (B), and (C) XRD pattern of TiO<sub>2</sub>/Ti Plate

**Fig. 2** **A** Surface morphology of the TiO<sub>2</sub>/Ti electrode, and **B** Surface morphology of the Te–TiO<sub>2</sub>/Ti electrode, **C** EDX elemental spectrum of Te–TiO<sub>2</sub>/Ti electrode and **D** FTIR spectrum of Te–TiO<sub>2</sub>/Ti electrode



be beneficial for surface reaction during photocatalytic or photoelectrocatalytic degradation of dye due to the large area of the active site. However, the surface morphology of the Te–TiO<sub>2</sub> electrode is very different from the TiO<sub>2</sub> layer morphology (Fig. 2B). This could be the result of the surface modification during the Te doping process of TiO<sub>2</sub>/Ti electrode that alters the tubular morphology of the surface. The formation of the Te layer on the top surface of the TiO<sub>2</sub>/Ti electrode that covers the tubular structure of the TiO<sub>2</sub>/Ti surface could also be considered for the modification of the surface structure of the electrode. As we can see from the image that the surface is now composed of a chunk structure that constructs the entire surface. The size of the chunk can be up to 9 μm. Nevertheless, owing to the in-compact arrangement of the chunks on the surface, they produce a highly porous film, which provides a large area of active sites for highly efficient surface reaction.

To verify the existence of Te doping on the TiO<sub>2</sub> film, we carried out EDX analysis on the sample. The result is shown in Fig. 2C. As the figure shows, the element of Te appears in the EDX spectrum at a binding energy of 3.7 keV, which is correspondent to L $\alpha$  mode excitation of Te electron energy level, along with the peaks of TiO<sub>2</sub> film background. The atomic composition of the Te element in the film is also significantly high with a typical concentration of 2.48 atomic %. This result certainly is strong evidence that the Te doping process on the TiO<sub>2</sub> film is successfully achieved. Nevertheless, to further confirm the nature of Te doping into the TiO<sub>2</sub>, we performed FTIR analysis on the sample. The result is shown in Fig. 2D. We can see from the FTIR spectrum that

the Te presence in the sample is indicated by the absorption peak at 750 cm<sup>-1</sup>, which is attributed to the Te–O vibration signature [32, 33]. Meanwhile, the Ti–O bond signature is observed at 400–1250 cm<sup>-1</sup> wavenumber with an absorption peak at 1083 cm<sup>-1</sup> area. Along with the Ti–O and Te–O bonds vibration mode, we also observed other vibration spectrums related to O–H, C–O, and C–H alkanes. The O–H bond, derived from water vapor on TiO<sub>2</sub> crystals, appears in the wavenumber of 3200 cm<sup>-1</sup> – 3600 cm<sup>-1</sup> with absorption peaks at 3381 cm<sup>-1</sup>. The C–H alkane bond that is originated from acetic acid is shown at a wavelength of 3000 cm<sup>-1</sup> – 2850 cm<sup>-1</sup> with absorption peaks at 2939 cm<sup>-1</sup> and 2875 cm<sup>-1</sup> [34]. Meanwhile, the absorption peak of C–O is found at 1645 cm<sup>-1</sup> and 1700 cm<sup>-1</sup>. Although the co-existence of these vibrational modes, this phenomenon is normal and does not affect the intrinsic properties of the Te–TiO<sub>2</sub> sample.

### 3.2 Photoelectrocatalytic performance

We evaluated the photoelectrocatalytic properties of the prepared electrode by conducting linear sweep voltammetry (LSV) analysis in 0.1 M solution NaNO<sub>3</sub> under irradiation of UV and visible light. Figure 3 shows the typical LSV response of the Te–TiO<sub>2</sub>/Ti and TiO<sub>2</sub>/Ti electrode when being subjected to UV and visible light illumination. As the figure reveals, the TiO<sub>2</sub>/Ti electrode indicates active photoelectrocatalytic properties under irradiation of UV light, which is normal and has widely reported with similar behavior. As also shown in Fig. 3A, the TiO<sub>2</sub>/Ti electrode

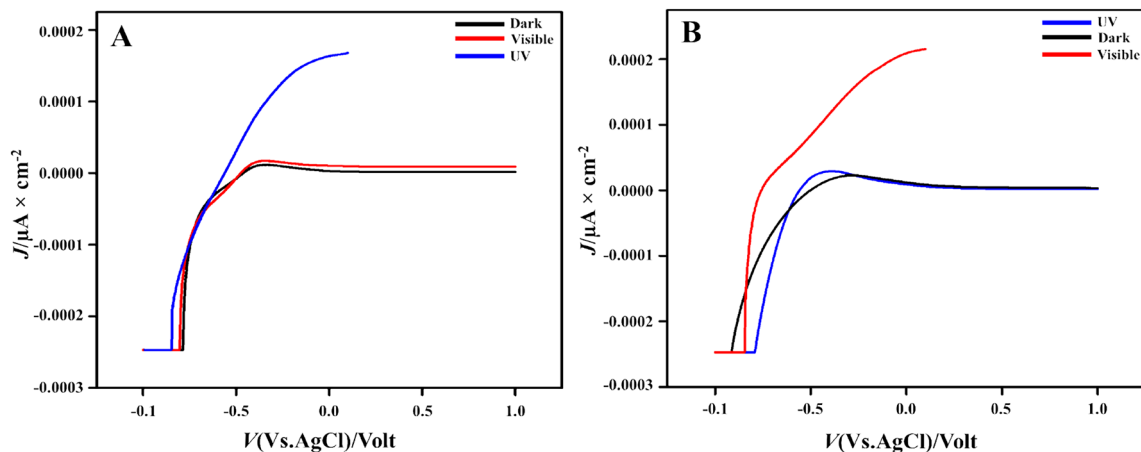


**Fig. 3** Linear Sweep Voltammetry (LSV) profile of  $\text{TiO}_2/\text{Ti}$  Electrodes (**A**) and  $\text{Te-TiO}_2/\text{Ti}$  (**B**) electrodes in 0.1 M solution  $\text{NaNO}_3$  under irradiation of UV and visible light irradiation

is not photoelectrocatalytically active when illuminated by a visible light source as that it produces a small current along with the potential windows. This response is more or less similar to the one recorded in the dark. To our surprise, the  $\text{Te-TiO}_2/\text{Ti}$  electrode shows highly active photoelectrocatalytic properties under visible irradiation that witness a high current increment during LSV measurement. Also to our surprise, the  $\text{Te-TiO}_2/\text{Ti}$  does not show a photoelectrocatalytic activity under UV irradiation where its LSV response is simply similar to the LSV under dark. The modification of the photoelectrocatalytic properties of the  $\text{Te-TiO}_2/\text{Ti}$  to visible is a strong verification of effective photoelectrical properties modification of  $\text{TiO}_2$  when being doped with Te cation. Thus, this electrode may be potential for cheap and efficient dye agent photoelectrocatalytic degradation under visible light.

We then evaluate the photoelectrocatalytic properties of the  $\text{Te-TiO}_2/\text{Ti}$  electrode in the degradation of Reactive yellow 105 dye. Figure 4 shows photoelectrocatalytic degradation kinetic of the dye under visible light irradiation. The figure also presents the degradation kinetic of dye under UV light irradiation. As the figure shows, as also expected, the photoelectrocatalytic degradation of dye is much more active under visible light irradiation where it can completely remove the dye within only 60 min time of reaction. For comparison, it is only 95% degradation under UV light irradiation. This is impressively higher than the performance demonstrated by the  $\text{TiO}_2/\text{Ti}$  where only 95% degradation under UV light irradiation and even much lower if under visible light irradiation (70%). This fact is certainly a piece of strong evidence that the  $\text{Te-TiO}_2/\text{Ti}$  electrode system can drive highly active degradation of dye activated by low

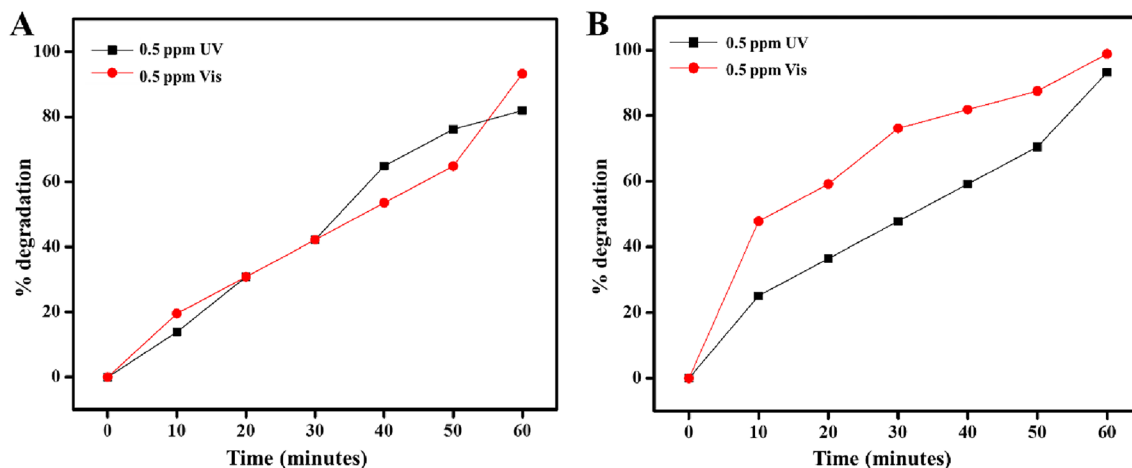


**Fig. 4** Photoelectrocatalytic degradation of Reactive yellow 105 compound using  $\text{TiO}_2/\text{Ti}$  (**A**) and  $\text{Te-TiO}_2/\text{Ti}$  (**B**) electrodes under UV and visible light irradiation

energy visible light irradiation, enabling facile and cheap dye contamination eradication. And even, the present photocatalytic system far outperforms the performance that is demonstrated by other photocatalysts system, such as doped-ZnO nanostructures [35],  $\text{Al}_2\text{O}_3/\text{ZrO}_2$  nanocomposite [36] and  $\text{CuFe}_2\text{O}_4$  modified activated carbon [37] and a membrane-based system [38], in degrading the Reactive yellow 105 dye or other azo dye derivatives.

Photoelectrocatalytic oxidation kinetics of organic compounds are then fitted with the Langmuir-Hinshelwood (L-H) equation. Using this equation, we can determine the reaction rate constant by plotting the logarithmic natural of initial concentration over concentration at a certain reaction time,  $\ln(C_0/C_t)$ , versus the reaction time. The reaction rate constant ( $k$ ) is the slope of the curve. We found that the  $k$

value for the photoelectrocatalytic reaction in the presence of  $\text{Te-TiO}_2/\text{Ti}$  electrode under visible and UV light irradiation is  $0.0611$  and  $0.037 \text{ min}^{-1}$ , respectively. This value is doubly higher than the reaction using  $\text{TiO}_2/\text{Ti}$  electrode, of which it is only  $0.0299$  and  $0.0361 \text{ min}^{-1}$  in  $\text{TiO}_2/\text{Ti}$  electrode under visible and UV light irradiation respectively.

To understand the extent of the effect photoelectrocatalytic properties of  $\text{Te-TiO}_2/\text{Ti}$  electrode in the dye degradation, we examined the photolysis degradation kinetic of dye under UV and visible light irradiation in the absence of photocatalyst. The result is shown in Fig. 5. As can be seen from the figure, the UV and visible light irradiation can also degrade the dye where the dye degrades up to 42% under UV light irradiation and 32% under visible light irradiation. The degradation of dye molecules under light irradiation is normal in the process that it is the result of hydroxyl radical formation when water absorbs photon energy. In turn, the hydroxyl radical functions as an oxidizing agent to attack and degrade the dye molecules [39]. This process is light energy-dependent where a high energy light source may produce a high density of active radical in the solution for rapid dye molecules degradation, the phenomenon that is also observed in this study. One thing we should note here is that the visible-light-driven degradation in the absence of a catalyst is relatively low compared with the one shown in Fig. 4. This describes the excellent photoelectrocatalytic properties of the  $\text{Te-TiO}_2/\text{Ti}$  electrode.

While the photolysis degradation result explains the extent effect of light irradiation in degrading the dye molecules, we further evaluated the photocatalytic degradation of dye in the presence of  $\text{Te-TiO}_2/\text{Ti}$  and  $\text{TiO}_2/\text{Ti}$  photocatalyst and under irradiation of UV and visible light sources. Figure 6 A shows the corresponding photocatalytic degradation kinetics of dye molecules results. As the figure suggests, in good agreement with the result shown

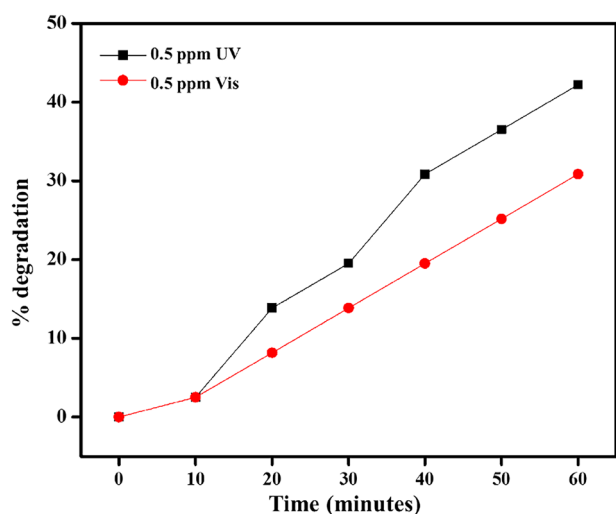


**Fig. 5** Photolysis degradation of Reactive yellow 105 under UV and visible light irradiation

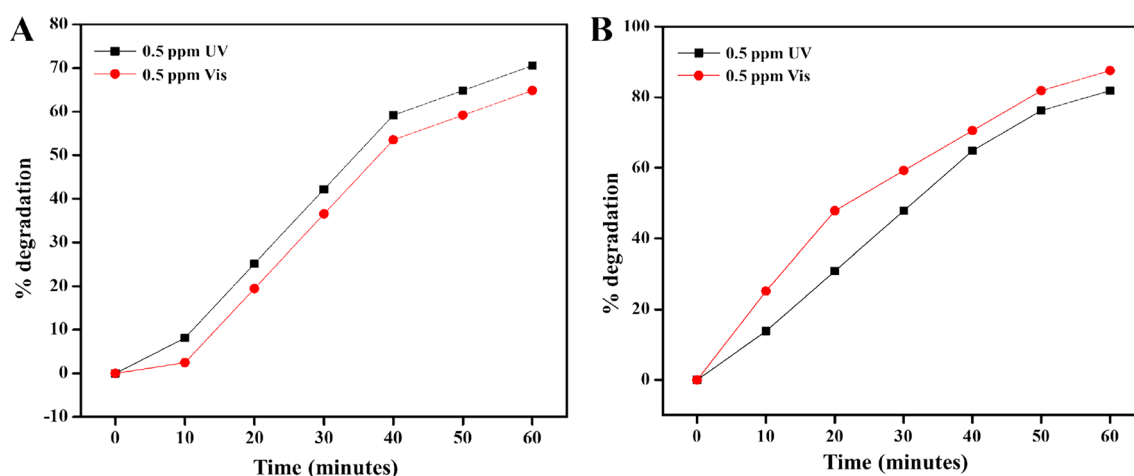


**Fig. 6** Photocatalytic degradation of Reactive yellow 105 over  $\text{TiO}_2/\text{Ti}$  (A) and  $\text{Te-TiO}_2/\text{Ti}$  (B) electrode under UV and visible light irradiation

in Fig. 6, the photocatalytic activity of Te–TiO<sub>2</sub>/Ti photocatalyst is much more energetic under visible irradiation than under UV light irradiation. In the typical result, we recorded the degradation up to 90% in the reaction driven by the visible light irradiation. Meanwhile, only 82% degradation is documented in the reaction influenced by UV light irradiation. For comparison, the photocatalytic degradation of dye is much lower in the reaction using TiO<sub>2</sub>/Ti photocatalyst (Fig. 6b) with photodegradation preference under UV light irradiation.

Based on these results, we remark that the Te–TiO<sub>2</sub>/Ti system offers highly active photoelectrocatalytic properties in the visible light activation the result of Te cation doping. Doping in many cases modifies the valence or conduction level density of state due to equilibrating of charge. In the case of Te with 6 valence electrons, it creates excess electrons in the TiO<sub>2</sub> system and forms an impurity level below the conduction band. With such a high density of state of the electron at the conduction band edge, it may be actively excited to the conduction band by the visible light energy and then react with water to produce hydroxyl radical. Such a circumstance of high-density hydroxyl radical in the reaction accelerates the degradation of dye molecules. Therefore, considering the simplicity of the materials preparation process and the unusual high performance of visible-driven photoelectrocatalytic activities, the Te–TiO<sub>2</sub>/Ti system should become a potential platform for environmental contamination control.

## 4 Conclusion

The synthesis and the evaluation of the photoelectrocatalytic activity of Te doped TiO<sub>2</sub>/Ti in the degradation of Reactive yellow 105 dye agents have been carried out. Elemental analysis and FTIR spectroscopy results have verified the successfulness of the Te doping into the TiO<sub>2</sub>/Ti matrix with doping atomic percent as high as 2.48%. The Te–TiO<sub>2</sub>/Ti electrode exhibits highly active photoelectrocatalytic properties under visible light excitation, witnessing the complete degradation of 0.5 ppm Reactive yellow 105 dye within 60 min time of reaction with degradation rate constant as high as 0.0611 M<sup>-1</sup> min<sup>-1</sup>. This value is doubly higher if compared to its photoelectrocatalytic activity under UV light irradiation or to undoped TiO<sub>2</sub>/Ti electrode under UV light irradiation of which their degradation rate constants are only as low as 0.037 and 0.0361 M<sup>-1</sup> min<sup>-1</sup>, respectively. We assumed that the visible light-driven activities are the result of increased electron density of state at the conduction band edge upon being doped with Te. The Te doped TiO<sub>2</sub>/Ti photoelectrocatalyst can be a new platform for rapid Reactive yellow 105 dye contamination in the environment.

**Acknowledgements** We acknowledge the financial support from the Ministry of Education and Culture of the Republic of Indonesia under the Basic Research award Grant No SP-DIPA-023.17.1.690523/2022, 51/UN29.20/PG/2022 and World Class Professor award Grant No 3252/E4/DT.04.03/2022. The authors are also grateful for the financial support from the Universiti Kebangsaan Malaysia under Dana Impact Perdana Grant No DIP-2021-025.

## References


- Nurdin M, Muzakkar MZ, Maulidiyah M et al (2016) *J Mater Environ Sci* 7:3334–3343
- Muzakkar MZ, Natsir M, Alisa A et al (2021) Photoelectrocatalytic degradation of reactive red 141 using FeTiO<sub>3</sub> composite doped TiO<sub>2</sub>/Ti electrodes. *J Phys: Conf Ser* 1899:012043
- Bijarimi M, Shahadah N, Ramli A et al (2020) *Indones J Chem* 20:276–281
- Mahmoud ME, Nabil GM, El-Mallah NM, Karar SB (2015) *Desalin Water Treat* 55:227–240
- Roy Choudhury AK (2014) Environmental impacts of the textile industry and its assessment through life cycle assessment. In: Muthu SS (ed) *Roadmap to sustainable textiles and clothing: environmental and social aspects of textiles and clothing supply chain*. Springer Singapore, Singapore
- Amalraj A, Pius A (2015) Photodegradation of reactive red 141 and reactive yellow 105 dyes using prepared TiO<sub>2</sub> nanoparticles. *Mater Sci Forum* 807:65–79
- Zuorro A, Lavecchia R (2014) *Desalin Water Treat* 52:1571–1577
- Muzakkar MZ, Maulidiyah M, Ningsi N et al (2021) High photoelectrocatalytic activity of selenium (Se) doped TiO<sub>2</sub>/Ti electrode for degradation of reactive orange 84. *J Phys: Conf Ser* 1899:012046
- Azis T, Maulidiyah M, Muzakkar MZ et al (2021) *Surf Eng App Elec* 57:387–396
- Muzakkar MZ, Umar A, Ilham I et al (2019) *J Phys: Conf Ser* 1242:012016
- Nurdin M, Azis T, Maulidiyah M et al (2018) Photocurrent responses of metanil yellow and remazol red B organic dyes by using TiO<sub>2</sub>/Ti electrode. *IOP Conf Ser: Mater Sci Eng* 367:012048
- Zhang Q, Wang H, Fan X et al (2016) *Surf Coat Technol* 298:45–52
- Maulidiyah M, Ritonga H, Salamba R et al (2015) *Int J ChemTech Res* 8:645–653
- Dzinun H, Othman MHD, Ismail AF et al (2015) *Chem Eng J* 269:255–261
- Muzakkar MZ, Azis T, Rajiani M et al (2021) The effect of calcogenate sulfur on the performance of the S-TiO<sub>2</sub>/Ti electrode as a photoelectrocatalytic sensor for phenolic compounds. *J Phys: Conf Ser* 1763:012069
- Nurdin M, Maulidiyah M, Muzakkar MZ, Umar AA (2019) *Microchem J* 145:756–761
- Sun Q, Xu Y (2010) *J Phys Chem* 114:18911–18918
- Wibowo D, Muzakkar MZ, Saad SKM et al (2020) *J Photochem Photobiol A: Chem* 398:112589
- Purnama A, Priatmoko S, Wahyuni S (2013) *Indones J Chem Sci* 2:3
- Irwan I, Muzakkar MZ, Umar A et al (2021) Effect of hexamethylenetetramine surfactant in morphology and optical properties of TiO<sub>2</sub> nanoparticle for dye-sensitized solar cells. *J Phys: Conf Ser* 1899:012045
- Al-She'irey AYA, Saad SKM, Umar AA et al (2016) *J Alloys Compd* 674:470–476

22. Shirsath S, Pinjari D, Gogate P et al (2013) *Ultrason Sonochem* 20:277–286
23. Saad SKM, Umar AA, Rahman MYA, Salleh MM (2015) *Appl Surf Sci* 353:835–842
24. Umar A, Rahman M, Saad S et al (2013) *Appl Surf Sci* 270:109–114
25. Saad SKM, Umar AA, Nguyen HQ et al (2014) *RSC Adv* 4:57054–57063
26. Nurdin M, Darmawati D, Maulidiyah M, Wibowo D (2018) *J Coat Technol Res* 15:395–402
27. Zhao K, Wu Z, Tang R, Jiang Y (2013) *J Korean Chem Soc* 57:489–492
28. Azis T, Nurwahidah AT, Wibowo D, Nurdin M (2017) *Environ Nanotechnol. Monit Manage* 8:103–111
29. Maulidiyah M, Wibowo D, Herlin H et al (2017) *Asian J Chem* 29:2504–2508
30. Liu D, Tian R, Wang J et al (2017) *Chemosphere* 185:574–581
31. Bijarimi M, Ahmad S, Rasid R et al (2016) Poly (lactic acid)/Poly (ethylene glycol) blends: mechanical, thermal and morphological properties. *Rev Prog Quant Nondestruct Eval*. <https://doi.org/10.1063/1.4945957>
32. Azis T, Maulidiyah M, Natsir M et al (2021) *Technol Rep Kansai Univ* 63:7611–7621
33. Muzakkar MZ, Nurdin M, Ismail I et al (2019) *Emiss Control Sci Technol* 3:1–9
34. Jagadale TC, Takale SP, Sonawane RS et al (2008) *J Phys Chem* 112:14595–14602
35. Christy EJS, Amalraj A, Rajeswari A, Pius A (2021) *Environ Chem Ecotoxicol* 3:31–41
36. Yaghoubi A, Ramazani A, Taghavi Fardood S (2020) *ChemistrySelect* 5:9966–9973
37. Xiao J, Fang X, Yang S et al (2015) *J Chem Technol Biotechnol* 90:1861–1868
38. Rajeswari A, Jackcina Stobel Christy E, Pius A (2018) *J Photochem Photobiol B: Biol* 179:7–17
39. Nurdin M, Darmawati D, Maulidiyah M, Wibowo D (2018) *J Coat Technol Res* 15:395–402

**Publisher's Note** Springer Nature remains neutral with regard to jurisdictional claims in published maps and institutional affiliations.

Springer Nature or its licensor holds exclusive rights to this article under a publishing agreement with the author(s) or other rightsholder(s); author self-archiving of the accepted manuscript version of this article is solely governed by the terms of such publishing agreement and applicable law.

## Authors and Affiliations

Muhammad Nurdin<sup>1</sup> · Muhammad Zakir Muzakkar<sup>1</sup> · Maulidiyah Maulidiyah<sup>1</sup> · Cici Sumarni<sup>1</sup> · Thamrin Azis<sup>1</sup> · Ratna Ratna<sup>2</sup> · Muhammad Natsir<sup>1</sup> · Irwan Irwan<sup>1,4</sup> · La Ode Agus Salim<sup>1,5</sup> · Akrajas Ali Umar<sup>3</sup> 

✉ Muhammad Nurdin  
mnurdin06@yahoo.com

✉ Akrajas Ali Umar  
akrajas@ukm.edu.my

<sup>1</sup> Department of Chemistry, Faculty of Mathematics and Natural Sciences, Universitas Halu Oleo, Kendari, Southeast Sulawesi 93232, Indonesia

<sup>2</sup> Chemistry Education Department, Teacher Training and Education Faculty, Universitas Halu Oleo, Kendari, Southeast Sulawesi 93232, Indonesia

<sup>3</sup> Institute of Microengineering and Nanoelectronics, Universiti Kebangsaan Malaysia (UKM), Selangor 43600 Bangi, Malaysia

<sup>4</sup> Department of Pharmacy, Faculty of Sciences and Technology, Institut Teknologi dan Kesehatan Avicenna, Kendari, Indonesia

<sup>5</sup> Department of Chemistry, Faculty of Science Technology and Health, Institut Sains Teknologi dan Kesehatan (ISTEK) 'Aisyiyah Kendari, Kendari, Indonesia